

Figure 2. Correlation between ΔV^* and ΔV for the aquation of $\text{Co}(\text{NH}_3)_5(\text{RCOO})^{2+}$ and $\text{Co}(\text{NH}_3)_5(\text{RCOOH})^{3+}$.

This is quite analogous to the correlation pointed out by Lawrance in the case of 11 neutral ligands X^0 :⁵

$$\bar{V}^\circ(\text{Co}(\text{NH}_3)_5\text{X}^{3+}) = (1.0 \pm 0.03)[\bar{V}^\circ(\text{X}^0)] + (37.0 \pm 1.6) \quad (19)$$

These correlations have a gradient of unity and demonstrate the additivity of \bar{V}° values of the pentaamminecobalt(III) complex. The intercept of eq 19 is significantly lower than that of eq 18. This reflects the strong electrostriction due to the 3+-charged complex. The magnitude of ΔV in Table V is slightly negative for the neutral leaving ligand RCOOH, whereas it is significantly negative for the uninegative leaving ligand RCOO⁻. This tendency also demonstrates the role of electrostriction.¹⁹ In the former,

the charge on the complex is conserved during the reaction, whereas in the latter charge separation occurs and electrostriction is enhanced. The ΔV^* values in Table V are obtained at 65–80 °C, whereas the ΔV values are obtained at 25 °C. Recently, we have obtained the ΔV^* value of reaction 1 for $\text{X} = \text{Cl}^-, \text{Br}^-, \text{NO}_3^-$ at relatively high temperatures (40–65 °C).²⁰ The results were similar to those already known at 25 °C, and the temperature effect on the ΔV^* values of these reactions is not significant. Therefore, neglecting the temperature effect on ΔV^* , we can check the applicability of eq 2. As illustrated in Figure 2, the data points are fairly close to the line representing eq 2. Thus, eq 2 is also valid for these reactions treated in the present work. Alternatively, when the present results are combined with previous ones, a correlation can be obtained:

$$\Delta V^* = (0.48 \pm 0.02)\Delta V + (1.5 \pm 0.3) \quad (20)$$

Equation 20 is essentially analogous to eq 2. According to the consideration as given in the Introduction, eq 20 underlines the interchange character for the 24 aquations of $\text{Co}(\text{NH}_3)_5\text{X}^{n+}$.

Registry No. $\text{Co}(\text{NH}_3)_5(\text{HCOO})^{2+}$, 19173-64-9; $\text{Co}(\text{NH}_3)_5(\text{CH}_3\text{COO})^{2+}$, 16632-78-3; $\text{Co}(\text{NH}_3)_5(\text{C}_2\text{H}_5\text{COO})^{2+}$, 19173-62-7; $\text{Co}(\text{NH}_3)_5(\text{CH}_2\text{ClCOO})^{2+}$, 19173-67-2; $\text{Co}(\text{NH}_3)_5(\text{CH}_2\text{BrCOO})^{2+}$, 19173-69-4; $\text{Co}(\text{NH}_3)_5(\text{CHCl}_2\text{COO})^{2+}$, 19173-68-3; $\text{Co}(\text{NH}_3)_5(\text{CHBr}_2\text{COO})^{2+}$, 19173-70-7; $\text{Co}(\text{NH}_3)_5(\text{CCl}_3\text{COO})^{2+}$, 19998-53-9; $\text{Co}(\text{NH}_3)_5(\text{CF}_3\text{COO})^{2+}$, 19173-66-1; $[\text{Co}(\text{NH}_3)_5\text{H}_2\text{O}](\text{ClO}_4)_3$, 13820-81-0; $\text{CH}_2\text{ClCOONa}$, 3926-62-3; $\text{CHCl}_2\text{COONa}$, 2156-56-1; CCl_3COONa , 650-51-1; CF_3COONa , 2923-18-4; $\text{CHBr}_2\text{COONa}$, 631-64-1; $\text{CH}_2\text{BrCOONa}$, 79-08-3.

(19) Hamann, S. D. *Rev. Phys. Chem. Jpn.* **1980**, *50*, 147–168.

(20) Kitamura, Y.; et al., to be submitted for publication.

Contribution from the Departments of Chemistry, University of Cincinnati, Cincinnati, Ohio 45221, and Rosary College, River Forest, Illinois 60305, and Chemistry Division, Argonne National Laboratory, Argonne, Illinois 60439

Electron-Transfer Reactions of Technetium and Rhenium Complexes. 2.¹ Relative Self-Exchange Rate of the M(I)/M(II) Couples $[\text{M}(\text{DMPE})_3]^{+/2+}$, Where M = Tc or Re and DMPE = 1,2-Bis(dimethylphosphino)ethane

Karen Libson,² Mary Woods,³ James C. Sullivan,⁴ J. W. Watkins II,² R. C. Elder,² and Edward Deutsch*²

Received April 27, 1987

The relative rates of self-exchange of the closely related d⁶/d⁵ couples $[\text{Tc}(\text{DMPE})_3]^{+/2+}$ and $[\text{Re}(\text{DMPE})_3]^{+/2+}$ have been determined by two independent applications of the Marcus theory. (1) The rates and equilibrium constants governing the cross-reactions between $[\text{Re}(\text{DMPE})_3]^+$ and $[(\text{NH}_3)_5\text{RuL}]^{3+}$ (L = 4-picoline, pyridine, and isonicotinamide) were measured in a 0.100 M LiCl and 0.001 M HCl aqueous medium and compared to equivalent data previously obtained for the reaction of $[\text{Tc}(\text{DMPE})_3]^+$ with the same three Ru(III) complexes in this medium. Independent electrochemical measurements show that in this medium the difference in reduction potential $E_{\text{Tc}^{0+}} - E_{\text{Re}^{0+}}$ is 80 ± 2 mV. Application of the Marcus cross relationship to these data leads to three independently determined values of $k_{\text{ex}}^{\text{Re}}/k_{\text{ex}}^{\text{Tc}}$: 2.1 ± 0.3, 1.3 ± 0.2, and 3.2 ± 0.8 for the 4-picoline, pyridine, and isonicotinamide complexes, respectively. The weighted average of these determinations, 1.6 ± 0.2, provides the best composite estimate of the kinetically determined $k_{\text{ex}}^{\text{Re}}/k_{\text{ex}}^{\text{Tc}}$ ratio. (2) EXAFS measurements were used to obtain average Re(I)–P and Re(II)–P bond lengths for the $[\text{Re}(\text{DMPE})_3]^{+/2+}$ complexes, and these data were compared to equivalent data available for the $[\text{Tc}(\text{DMPE})_3]^{+/2+}$ complexes. The difference in bond lengths, (M^{II}–P) – (M^I–P), is less for the Re couple than for the Tc couple (0.054 vs 0.068 Å), and within the Marcus formalism this leads directly to a structurally determined value of $k_{\text{ex}}^{\text{Re}}/k_{\text{ex}}^{\text{Tc}} = 2$. Thus, the kinetically observed, slightly greater rate of self-exchange of the $[\text{Re}(\text{DMPE})_3]^{+/2+}$ couple is seen to be due entirely to the somewhat smaller structural distortions suffered by the inner coordination sphere of the Re complex during electron transfer. The absolute self-exchange rates of the $[\text{Re}(\text{DMPE})_3]^{+/2+}$ and $[\text{Tc}(\text{DMPE})_3]^{+/2+}$ couples are calculated to be 4 × 10⁶ M⁻¹ s⁻¹ and 2 × 10⁶ M⁻¹ s⁻¹, respectively (25 °C, μ = 0.10 M).

Introduction

During the past 3 decades there has been considerable interest in determining the rates of self-exchange reactions for outer-sphere redox couples, and in providing a theoretical framework for un-

derstanding these fundamental electron transfer reactions.⁵ Despite the extensive compilation of experimentally determined self-exchange rates that has resulted from this interest, there are no examples known to us that meet the following criteria: (i) identical experimental procedures and conditions are used to determine the relative E° values and self-exchange rates of two analogous redox couples, the central metals of which are second-

(1) Part 1: Doyle, M. N.; Libson, K.; Woods, M.; Sullivan, J. C.; Deutsch, E. *Inorg. Chem.* **1986**, *25*, 3367.

(2) University of Cincinnati.

(3) Rosary College.

(4) Argonne National Laboratory.

(5) Marcus, R. A.; Sutin, N. *Biochim. Biophys. Acta* **1985**, *811*, 265.

and third-row group congeners; (ii) all four complexes of the two redox couples are structurally characterized. Such examples would provide a more stringent test of electron-transfer theory than is now possible since the analogous components of such redox couples will have essentially the same overall size, shape, and charge, and thus to a large extent it will be solely changes in the inner coordination spheres that determine the relative self-exchange rates of the two couples. To provide such an example, we have determined the $E^{\circ'}$ value and electron-transfer kinetics of $[\text{Re}(\text{DMPE})_3]^{+/2+}$ by using the same experimental procedures and conditions employed in our previous study¹ of $[\text{Tc}(\text{DMPE})_3]^{+/2+}$, and have utilized EXAFS to determine the Re-P bond lengths in the component complexes. The resulting kinetic and structural data are analyzed within the Marcus-Hush formalism for outer-sphere electron-transfer reactions in order to assess and explicate the relative self-exchange rates of the analogous $[\text{M}(\text{DMPE})_3]^{+/2+}$ ($\text{M} = \text{Tc}, \text{Re}$) couples.

An additional goal of this study was the assessment of the potential utility of the $[\text{Re}(\text{DMPE})_3]^{+/2+}$ couple for characterizing other redox systems. This couple enjoys the same attractive features as does the technetium analogue¹ (accessible redox potential, stability in both acidic and alkaline media, solubility in both aqueous and nonaqueous media, easily monitored spectrophotometric change, t_{2g} electron transfer, etc.) but does not suffer the disadvantage of involving a radioactive element.

Experimental Section

Materials. Triply recrystallized $[\text{Re}(\text{DMPE})_3]\text{F}_3\text{CSO}_3$, suitable for kinetic investigations, was available from a previous study which detailed the preparation, purification and properties of this salt.⁶ Solutions of $[\text{Re}(\text{DMPE})_3]^{+/2+}$ were calibrated spectrophotometrically ($\epsilon_{252} = 17\,200 \text{ M}^{-1} \text{ cm}^{-1}$).⁶ The Re(II) analogue $[\text{Re}(\text{DMPE})_3](\text{F}_3\text{CSO}_3)_2$ was prepared by H_2O_2 oxidation of the Re(I) complex in acetonitrile containing $\text{F}_3\text{CSO}_3\text{H}$; precipitation with water, followed by recrystallization from acetonitrile led to translucent red crystals of the desired material.⁷ Visible-UV in CH_3CN (λ , nm (ϵ , $\text{M}^{-1} \text{ cm}^{-1}$): λ_{max} 527 (1360), 416 (130), 340 (310), 234 (8710); λ_{sh} 484, 270; λ_{min} 431 (115), 376 (25), 335 (8300)). Recrystallized samples of the pentaammineruthenium(III) salts $[(\text{NH}_3)_5\text{RuL}](\text{F}_3\text{CSO}_3)_3$ with L = isonicotinamide, pyridine, or 4-picoline, were available from a previous study,¹ and solutions of these complexes were calibrated as previously described.¹ All other reagents used in the kinetic experiments were the same as previously detailed.¹

Procedures and Equipment. All procedures and equipment used in the kinetic studies were the same as previously described.¹ The $E^{\circ'}$ values for the $[\text{Tc}(\text{DMPE})_3]^{+/2+}$ and $[\text{Re}(\text{DMPE})_3]^{+/2+}$ couples were determined in the medium used for kinetic studies (0.100 M LiCl, 0.001 M HCl) by both cyclic voltammetry and differential-pulse polarography. For both determinations, measurements were done consecutively versus the same reference electrode in order to minimize the error in the difference $E_{\text{Tc}}^{\circ'} - E_{\text{Re}}^{\circ'}$. For each complex, the resulting independently determined $E^{\circ'}$ values are in good agreement with each other and with previously published values.^{1,6,8}

Powdered samples of $[\text{Re}^{\text{I}}(\text{DMPE})_3][\text{F}_3\text{CSO}_3]$ and $[\text{Re}^{\text{II}}(\text{DMPE})_3][\text{F}_3\text{CSO}_3]_2$ were prepared for the EXAFS analysis by dilution with Li_2CO_3 . The X-ray absorption spectra were recorded at the Stanford Synchrotron Radiation Laboratory (SSRL) on wiggler beam line IV-1 as previously described.⁸ A Si(220) double-crystal monochromator and standard nitrogen-filled ion chambers were used for transmission measurements. Fluorescence data were collected concurrently with a detector of the Stearn, Heald type⁹ purchased from the EXAFS Co., Seattle, WA. A copper-foil filter was used in the fluorescence detector to discriminate against scattered radiation. Wavelength calibration was accomplished by the simultaneous measurement of the spectrum of powdered rhenium metal. The energy range for data collection spanned 10.1–11.6 KeV, encompassing the Re L_{III} absorption edge. A total of 220 data points were collected beyond the edge at evenly spaced intervals in k -space with integration times varying from 1 to 12 s/point, the longer times being used for the points farther from the edge. Three scans were collected for each sample and then were averaged together for processing.

Table I. Calculated Second-Order Rate Parameters Governing the Reaction of $[\text{Re}^{\text{I}}(\text{DMPE})_3]^{+/2+}$ with $[(\text{NH}_3)_5\text{Ru}^{\text{III}}\text{L}]^{3+}$ Complexes^a

L^a	$T, ^\circ\text{C}$	no. of indep data sets	no. of indiv kinetic runs	$10^{-6} k^{2\text{nd}}, \text{M}^{-1} \text{s}^{-1}$
pic	25.0	6	35	2.1 ± 0.2
py	25.0	2	11	2.7 ± 0.2
isn	25.0	2	11	26 ± 6
pic	0	1	4	0.37 ± 0.02
py	0	1	3	0.62 ± 0.04
isn	0	1	5	14.5 ± 1.2

^a pic = 4-picoline; py = pyridine; isn = isonicotinamide; DMPE = 1,2-bis(dimethylphosphino)ethane.

Table II. Comparative Rate and Activation Parameters Governing the Reaction of $[\text{M}^{\text{I}}(\text{DMPE})_3]^{+/2+}$ ($\text{M} = \text{Tc}, \text{Re}$) Complexes with $[(\text{NH}_3)_5\text{Ru}^{\text{III}}\text{L}]^{3+}$ Complexes

L^a	M	$10^{-6} k^{2\text{nd}}, \text{M}^{-1} \text{s}^{-1}$	$\Delta H^\ddagger, \text{kcal/mol}$	$\Delta S^\ddagger, \text{eu}$
pic	Tc	0.30 ± 0.01	8.5 ± 0.1	-5 ± 1
pic	Re	2.1 ± 0.2	10.6 ± 0.7	$+6 \pm 2$
py	Tc	0.53 ± 0.01	5.1 ± 0.4	-15 ± 1
py	Re	2.7 ± 0.2	9.0 ± 0.6	$+1 \pm 2$
isn	Tc	3.57 ± 0.06	4.8 ± 1.5	-12 ± 5
isn	Re	26 ± 6	3.3 ± 1.7	-13 ± 6

^a Ligand abbreviations are defined in Table I. ^b 25 $^\circ\text{C}$.

Kinetics. Reactions were monitored at the characteristic absorption maximum of the Ru(II) product.¹ Concentrations of the Ru(III) reagent varied from 9×10^{-6} to $144 \times 10^{-6} \text{ M}$, while concentrations of $[\text{Re}(\text{DMPE})_3]^{+/2+}$ varied from 3×10^{-6} to $12 \times 10^{-6} \text{ M}$. The Ru(III) reagent was always in excess, and the Ru(III)/Re(I) ratio varied from 3 to 19. Replicate absorbance vs time data sets were collected for each unique combination of Ru(III) and Re(I) stock solutions. Rate constants and associated standard deviations were calculated for each replicate data set by using nonlinear least-squares techniques.

Kinetic Data Analysis. The equilibrium constants governing reaction of $[\text{Re}(\text{DMPE})_3]^{+/2+}$ with the three Ru(III) complexes are sufficiently large (vide infra) so that this reaction proceeds to completion and can be satisfactorily described by the rate law

$$d[\text{Ru}^{\text{II}}]/dt = k^{2\text{nd}}[\text{Re}^{\text{I}}][\text{Ru}^{\text{III}}]$$

Reductions of the picoline and pyridine complexes proceed sufficiently slowly so that they may be studied under pseudo-first-order conditions. For these reactions, individual observed first-order rate constants were calculated by using the usual exponential relationship. For each Ru complex, under all concentration conditions but at a given temperature, these individual first-order rate parameters were converted to second-order rate constants by applying the relationship

$$k^{2\text{nd}} = k_{\text{obsd}}^{1\text{st}} / ([\text{Ru}^{\text{III}}] - [\text{Re}^{\text{I}}] / 2)$$

where $([\text{Ru}^{\text{III}}] - [\text{Re}^{\text{I}}] / 2)$ is the average concentration of Ru(III) during the reaction, and the resulting individual values of $k^{2\text{nd}}$ were averaged. Reduction of the isonicotinamide complex proceeds so rapidly that it must be studied under second-order conditions. For this reaction, individual observed second-order rate constants were directly calculated from the absorbance vs time data and then averaged at each temperature.

Activation parameters for each reaction were estimated by linear analysis within the Eyring formalism. All quoted errors are standard deviations.

EXAFS Data Analysis. The details of the EXAFS data analysis have been reported previously.^{8,10} Typically a k range of 3–16 \AA^{-1} was used for the Fourier transformation. From the Fourier transform, an R range, in \AA space, was chosen to encompass the Re-P frequency component for back-transformation to k -space. These Fourier-filtered data, weighted by k^3 , were used for the curve-fitting analysis for the range 4–15 \AA^{-1} . The structural parameters were extracted by using the expression

$$X(k) = \frac{AN(F(k))(\exp(-2\sigma^2 k^2))(\sin(2kr + \phi(k)))}{kr^2}$$

where A is a scale factor, N is the number of atoms at the distance r contributing to the back scattering, k is the photoelectron wave vector,

- (6) Deutsch, E.; Libson, K.; Vanderheyden, J.-L.; Ketring, A. R.; Maxon, H. R. *Nucl. Med. Biol.* **1986**, *13*, 465.
 (7) Vanderheyden, J.-L. Ph.D. Thesis, University of Cincinnati, 1985.
 (8) Vanderheyden, J.-L.; Ketring, A. R.; Libson, K.; Heeg, M. J.; Roecker, L.; Motz, P.; Whittle, R.; Elder, R. C.; Deutsch, E. *Inorg. Chem.* **1984**, *23*, 3184.
 (9) Stern, E. A.; Heald, S. M. *Rev. Sci. Instrum.* **1979**, *50*, 1579.

- (10) Elder, R. C.; Watkins, J. W., II. *Inorg. Chem.* **1986**, *25*, 223.

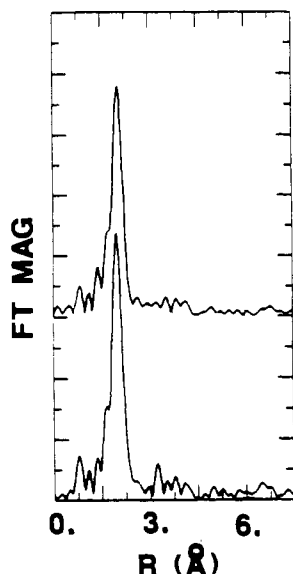


Figure 1. Fourier-transformed fluorescence EXAFS data for $k = 3\text{--}16 \text{ \AA}^{-1}$, plotted as the magnitude of the Fourier transform modulus versus phase-shifted distance (in \AA space). The lower trace is the FT of $[\text{Re}^{\text{I}}(\text{DMPE})_3]\text{F}_3\text{CSO}_3$ and the upper trace is the FT of $[\text{Re}^{\text{II}}(\text{DMPE})_3](\text{F}_3\text{CSO}_3)_2$.

Table III. Results of EXAFS Analysis

param	$[\text{Re}(\text{DMPE})_3]^+$	$[\text{Re}(\text{DMPE})_3]^{2+}$
r (\AA)	2.387 (10)	2.441 (10)
N	6.0 ^{a,b}	6.3
σ , (\AA)	0.038	0.054
ΔE_0	5.76	6.59
fit ^c	0.75	0.62
range, ^d \AA	1.47–2.46	1.52–2.47

^a Atom number fixed. ^b Scale factor of 0.36 determined from this fit. ^c Goodness of fit derived from $[\sum k^6(\chi_{\text{obsd}} - \chi_{\text{calcd}})^2/N]^{1/2}$, where N is the number of data points. ^d Range of back-transform for Fourier filters.

$F(k)$ is the backscattering amplitude function, σ^2 is the mean square deviation of r , and ϕ is the phase shift function for the absorber–scatterer pair (Re–P in this case). Theoretical functions for $F(k)$ and $\phi(k)$ are those of Teo and Lee¹¹.

Results

Table A¹² gives a complete listing of individual observed rate parameters, as a function of L , $[\text{Ru}(\text{III})]$, $[\text{Re}(\text{I})]$, and T , while Table I summarizes these data in the form of calculated average second-order rate parameters. Table II compares these data and the associated activation parameters to analogous data previously obtained¹ with $[\text{Tc}(\text{DMPE})_3]^+$.

Figure 1 shows the Fourier transforms of the fluorescence EXAFS data for $[\text{Re}^{\text{I}}(\text{DMPE})_3]\text{F}_3\text{CSO}_3$ and $[\text{Re}^{\text{II}}(\text{DMPE})_3](\text{F}_3\text{CSO}_3)_2$. Both transforms exhibit a symmetric peak occurring at 1.99 and 2.04 \AA for the Re(I) and Re(II) complexes, respectively. Thus a relatively symmetric distribution of phosphorus atoms about rhenium is indicated. The small shoulder occurring on the low- R side of the Re–P peak in the Fourier transform is likely to result from a nonlinear Re–P phase shift. Each peak (with shoulder) is isolated and back-transformed into k -space for the curve-fitting analysis. Figure 2 illustrates the best fit obtained for both of the rhenium complexes by using theoretical amplitude and phase functions. For the Re(I) complex, the coordination number was held fixed at 6.0 to determine the appropriate amplitude scale factor. The value of 0.36 thus determined was assumed to be transferable to the Re(II) complex for determination of the coordination number. The structural parameters obtained are listed in Table III.

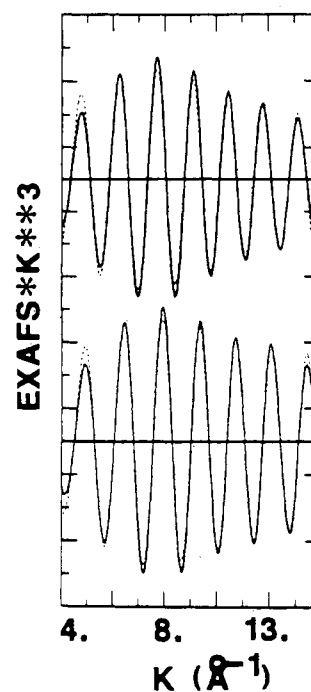


Figure 2. Plots of the Fourier-filtered EXAFS data and the best fit obtained by using theoretical Re–P amplitude and phase functions, plotted as the $\text{EXAFS} \times k^3$ vs k -space (in \AA^{-1}). The structural parameters obtained are given in Table III. The lower trace is the fit obtained for $[\text{Re}^{\text{I}}(\text{DMPE})_3]\text{F}_3\text{CSO}_3$ and the upper trace is the fit obtained for $[\text{Re}^{\text{II}}(\text{DMPE})_3](\text{F}_3\text{CSO}_3)_2$.

Table IV. Comparable Structural and Equilibrium Data for $[\text{M}(\text{DMPE})_3]^+$ ($M = \text{Tc}, \text{Re}$) Complexes^a

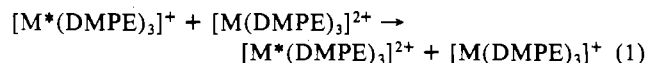
	Tc	Re
M(I)–P bond length, \AA	2.40 (1) ^b	2.387 (10)
M(II)–P bond length, \AA	2.468 (5) ^b	2.441 (10)
Δa° , \AA	0.068 (11)	0.054 (14)
E° for $[\text{M}(\text{DMPE})_3]^{2+} + e^-$, V vs NHE	0.290 (1) ^c	0.210 (1) ^c
K_{eq}^d for $[\text{M}(\text{DMPE})_3]^+ + [\text{A}_5\text{Ru}(\text{pic})]^{3+}$	0.39 (3)	8.8 (7)
K_{eq}^d for $[\text{M}(\text{DMPE})_3]^+ + [\text{A}_5\text{Ru}(\text{py})]^{3+}$	2.0 (2)	45 (4)
K_{eq}^d for $[\text{M}(\text{DMPE})_3]^+ + [\text{A}_5\text{Ru}(\text{isn})]^{3+}$	39 (3)	870 (70)

^a $\text{A} = \text{NH}_3$; other ligand abbreviations are defined in Table . Standard deviation of the last significant digit(s) is given in parentheses. ^b References 1 and 7. ^c E° determined in 0.100 M LiCl (0.001 M HCl). ^d Calculated from electrochemical data for $[\text{M}(\text{DMPE})_3]^{2+/+}$ (this table) and for $[\text{A}_5\text{RuL}]^{3+/2+}$ (ref 1).

Table IV summarizes comparable equilibrium and structural data for the $[\text{Re}(\text{DMPE})_3]^{+/2+}$ and $[\text{Tc}(\text{DMPE})_3]^{+/2+}$ couples. For the electrochemical data, the reported errors are based on comparable cyclic voltammometric and differential pulse polarographic experiments; the difference $E_{\text{Tc}}^\circ - E_{\text{Re}}^\circ$ can conservatively be taken to be 80 ± 2 mV. For the EXAFS data, the reported errors are based on comparisons between bond lengths determined by EXAFS and by single-crystal X-ray structural analyses.⁸

Discussion

Relative Rates of Self-Exchange of $[\text{M}(\text{DMPE})_3]^{+/2+}$ Couples from Structural Data. According to Marcus theory,^{13–15} the rate constant governing the self-exchange reaction



can be predicted from a relation that includes the work required to bring the reactants together, w_r , the activation energies required

(11) Teo, B.-K.; Lee, R. A. *J. Am. Chem. Soc.* **1979**, *101*, 2815.

(12) Supplementary material.

(13) Marcus, R. A. *Annu. Rev. Phys. Chem.* **1964**, *15*, 155.

(14) Marcus, R. A.; Siders, P. In *Mechanistic Aspects of Inorganic Reactions*; Rorabacher, D. B., Endicott, J. F., Eds.; ACS Symposium Series 198; American Chemical Society: Washington, DC, 1982; Chapter 10.

(15) Brown, G. M.; Sutin, N. *J. Am. Chem. Soc.* **1979**, *101*, 883.

to rearrange the inner, ΔG_{in}^* , and outer, ΔG_{out}^* , coordination spheres of the reactants, and the collision frequency of neutral molecules in solution, Z .

$$k_{ex} = Z \exp[(-w_r + \Delta G_{in}^* + \Delta G_{out}^*)/RT] \quad (2)$$

The only variables affecting the magnitude of w_r , ΔG_{out}^* , and Z (at constant temperature) are the charges and overall sizes of the reaction complex. Since the charges and sizes of the $[M(\text{DMPE})_3]^{+/2+}$ ($M = \text{Tc}, \text{Re}$) complexes are essentially identical (Table IV), these three parameters will not affect the relative rates of exchange of the Tc and Re complexes. Thus, the only parameter of significance in determining the relative rates of exchange is ΔG_{in}^* , which is given by

$$\Delta G_{in}^* = \frac{3\bar{f}(\Delta a^\circ)^2}{2} \quad (3)$$

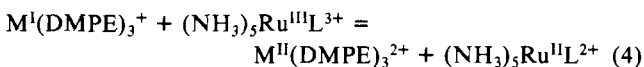
where \bar{f} represents the average force constant for the breathing vibrational modes of the reactant and product, and Δa° represents the difference between the radius of the reactant and that of the product. Values of Δa° are given in Table IV, while values of \bar{f} can be estimated from observed M–Cl stretching frequencies (ω) in $[\text{MCl}_6]^{2-}$ complexes (337 cm^{-1} for Tc^{16} and 346 cm^{-1} for Re^{17}) by using the relationship

$$\omega = \frac{(\bar{f}/\mu)^{1/2}}{2\pi c}$$

where μ is the reduced mass. It does not matter whether or not μ is corrected for the difference in mass between Cl and P since this correction is the same for both the Tc and Re complexes, and thus it does not significantly affect the calculated relative rate of exchange.

Equation 3 shows that the inner-sphere reorganization energy is governed by the ease of stretching the metal–ligand bond (\bar{f}) and the distance over which this bond must be stretched (Δa°). The fact that a Tc–ligand bond can be stretched more easily than a Re–ligand bond (\bar{f} values of 1.75×10^5 and $2.10 \times 10^5 \text{ dyn/cm}$, respectively) is more than offset by the fact that the Tc–P bond must be stretched further than the Re–P bond (Δa° values of 0.068 and 0.054 \AA , respectively). ΔG_{in}^* for the $[\text{Tc}(\text{DMPE})_3]^{+/2+}$ self-exchange is calculated to be 0.41 kcal/mol greater than that for the $[\text{Re}(\text{DMPE})_3]^{+/2+}$ reaction, corresponding to a relative rate of self-exchange, $k_{ex}^{\text{Re}}/k_{ex}^{\text{Tc}}$, of 2.0. Thus, a purely ground-state, structural analysis within the Marcus formalism predicts that the self-exchange rate of the $[\text{Re}(\text{DMPE})_3]^{+/2+}$ couple will be about twice as fast as the self-exchange rate of the analogous $[\text{Tc}(\text{DMPE})_3]^{+/2+}$ couple.

Relative Rates of Self-Exchange of $[\text{M}(\text{DMPE})_3]^{+/2+}$ ($M = \text{Tc}, \text{Re}$) Couples from Kinetic Data. The reactions of $[\text{Tc}(\text{DMPE})_3]^+$ and $[\text{Re}(\text{DMPE})_3]^+$ with the $[(\text{NH}_3)_5\text{Ru}^{\text{III}}\text{L}]^{3+}$ complexes are analogous in terms of stoichiometry and lack of acid dependence:



$M = \text{Tc}, \text{Re}; \text{L} = 4\text{-picoline, pyridine, isonicotinamide}$

Since the Re(I) complex is a stronger reductant than the Tc(I) analogue, the equilibrium shown in eq 4 lies further to the right for Re than it does for Tc (Table IV). This larger driving force for the Re(I) reduction is also manifested in the Re(I)–Ru(III) reactions being significantly faster than the analogous Tc(I)–Ru(III) reactions (Table II). The quantitative equilibrium and rate data of Tables IV and II can be used within the Marcus formalism to calculate the relative rates of self-exchange of the $[\text{M}(\text{DMPE})_3]^{+/2+}$ couples.

A modification^{1,5} of the theory underlying the Marcus cross relationships leads to the expression

$$k_{12}^2 = k_{11}k_{22}K_{12}f_{12}W_{12}^2 \quad (5)$$

where k_{12} is the rate of the cross-reaction between reagents 1 and 2 and K_{12} is the equilibrium constant governing this reaction, while k_{11} and k_{22} are the self-exchange rates of reagents 1 and 2, respectively, and f_{12} and W_{12} are defined by

$$\ln f_{12} = \frac{[\ln K_{12} + (w_{12} - w_{21})/RT]^2}{4 \left(\ln \frac{k_{11}k_{22}}{A_{11}A_{22}} + \frac{w_{11} + w_{22}}{RT} \right)} \quad (5a)$$

$$W_{12} = \exp[-(w_{12} + w_{21} - w_{11} - w_{22})/2RT] \quad (5b)$$

$$W_{ij} = \frac{z_i z_j e^2}{D_s r (1 + \kappa r)} \quad (5c)$$

$$\kappa = \left(\frac{8\pi N^2 e^2 \mu}{1000 D_s RT} \right)^{1/2} = \beta \mu^{1/2} \quad (5d)$$

D_s and n are the dielectric constant and refractive index of the medium, z_i is the charge of reactant i ; μ is the ionic strength, and β is the Debye–Hückel constant; consistent with previous estimates¹ we have taken $A_{11} = A_{22} = 2.8 \times 10^{12} \text{ M}^{-1} \text{ s}^{-1}$.

These equations are considerably simplified in the calculation of the relative rates of self-exchange of the $[\text{M}(\text{DMPE})_3]^{+/2+}$ couples.

$$(k_{12}^{\text{Tc/Ru}})^2 = (k_{ex}^{\text{Ru}} k_{ex}^{\text{Tc}} K_{12}^{\text{Tc/Ru}} f_{12}^{\text{Tc/Ru}}) (W_{12}^{\text{Tc/Ru}})^2 \quad (6a)$$

$$(k_{12}^{\text{Re/Ru}})^2 = (k_{ex}^{\text{Ru}} k_{ex}^{\text{Re}} K_{12}^{\text{Re/Ru}} f_{12}^{\text{Re/Ru}}) (W_{12}^{\text{Re/Ru}})^2 \quad (6b)$$

However, $W_{12}^{\text{Tc/Ru}} = W_{12}^{\text{Re/Ru}}$, since values of W_{12} depend only on the charges and sizes of the reactants and products and these are essentially identical for the Tc and Re complexes (Table IV). Also, since reactions with the same Ru complex are being compared, $k_{ex}^{\text{Ru}} = k_{ex}^{\text{Ru}}$ and thus

$$\frac{k_{ex}^{\text{Re}}}{k_{ex}^{\text{Tc}}} = \left(\frac{k_{12}^{\text{Re/Ru}}}{k_{12}^{\text{Tc/Ru}}} \right)^2 \left(\frac{K_{12}^{\text{Tc/Ru}}}{K_{12}^{\text{Re/Ru}}} \right) \frac{f_{12}^{\text{Tc/Ru}}}{f_{12}^{\text{Re/Ru}}} \quad (7)$$

Since the difference between $E_{\text{Tc}}^{\circ'}$ and $E_{\text{Re}}^{\circ'}$ is $80 \pm 2 \text{ mV}$ (Table IV), the ratio $K_{12}^{\text{Re/Ru}}/K_{12}^{\text{Tc/Ru}} = 22.5 \pm 1.7$ (at 25°C) independent of the identity of the ruthenium(III) complex and

$$\frac{k_{ex}^{\text{Re}}}{k_{ex}^{\text{Tc}}} = \left(\frac{k_{12}^{\text{Re/Ru}}}{k_{12}^{\text{Tc/Ru}}} \right)^2 \left(\frac{1}{22.5 \pm 1.7} \right) \frac{f_{12}^{\text{Tc/Ru}}}{f_{12}^{\text{Re/Ru}}} \quad (8)$$

Values of $k_{12}^{\text{Re/Ru}}$ and $k_{12}^{\text{Tc/Ru}}$ are given in Table II, while values of $f_{12}^{\text{Re/Ru}}$ and $f_{12}^{\text{Tc/Ru}}$ can be calculated from

$$\ln f_{12}^{\text{M/Ru}} = (\ln K_{12}^{\text{M/Ru}} - 0.371)/(-108.84) \quad (9)$$

which is obtained by substituting numerical values for the parameters in eq 5a, 5c, and 5d. Applying these values to eq 8 for each of the three ruthenium complexes studied leads to three independently determined values of $k_{ex}^{\text{Re}}/k_{ex}^{\text{Tc}}$: 2.1 ± 0.3 , 1.3 ± 0.2 , and 3.2 ± 0.8 for the 4-picoline, pyridine, and isonicotinamide complexes, respectively. The ratio derived from the isonicotinamide reaction is least precise since the reduction of $[(\text{NH}_3)_5\text{Ru}(\text{isn})]^{3+}$ by $[\text{Re}(\text{DMPE})_3]^+$ is so fast that it is at the limit of what can be monitored by the stopped-flow technique (Table I). The unweighted average of these three determinations is 2.2 ± 0.9 , but this calculation allows the least precise determination to dominate the error estimate. A more reasonably summary value of $k_{ex}^{\text{Re}}/k_{ex}^{\text{Tc}}$ is given by the weighted average, 1.6 ± 0.2 .

Comparison of Relative Rates of Self-Exchange from Structural and Kinetic Data. Both the structural and kinetic calculations of $k_{ex}^{\text{Re}}/k_{ex}^{\text{Tc}}$ clearly lead to the conclusion that the rates of self-exchange of the $[\text{M}(\text{DMPE})_3]^{+/2+}$ couples are very similar in magnitude but that the Re self-exchange rate is slightly faster than the Tc self-exchange rate. Both calculations indicate that the difference in rate is about a factor of 2, but the relatively large uncertainties inherent in the experimental parameters used in these calculations make it impossible to generate a more accurate as-

(16) Baluka, M.; Hanuza, J.; Jezowska-Trzbiatowska, B. *Bull. Acad. Pol. Sci., Ser. Sci. Chim.* 1972, 20, 271.

(17) Mohan, S.; Ravikumar, K. G. *Indian J. Pure Appl. Phys.* 1980, 18, 857.

Table V. Rates of Self-Exchange for the $[M(\text{DMPE})_3]^{+/2+}$ Couples ($M = \text{Tc, Re}$) Calculated from the Marcus Cross Relationship (Eq 5)^a

electron-transfer partner	$10^{-6} k_{\text{ex}}^{\text{Tc}}$	$10^{-6} k_{\text{ex}}^{\text{Re}}$	$k_{\text{ex}}^{\text{Re}}/k_{\text{ex}}^{\text{Tc}}$
$[\text{A}_5\text{Ru}(\text{pic})]^{3+/2+}$	1.48 ± 0.12	3.11 ± 0.36	2.1 ± 0.3
$[\text{A}_5\text{Ru}(\text{py})]^{3+/2+}$	0.89 ± 0.09	1.15 ± 0.13	1.3 ± 0.2
$[\text{A}_5\text{Ru}(\text{isn})]^{3+/2+}$	2.28 ± 0.18	7.4 ± 1.8	3.2 ± 0.8

^a $\text{A} = \text{NH}_3$; other ligand abbreviations are defined in Table I. Units on rate constants are $\text{M}^{-1} \text{s}^{-1}$ (25 °C).

essment.¹⁸ However, it is gratifying that when the effects of experimental errors are minimized by treating relative rates and closely related systems are studied, the Marcus formalism is sufficiently powerful to account for differences in self-exchange rates that are as small as a factor of 2.

Calculation of Absolute Rates of Self-Exchange from Kinetic Data. Parameters given in Tables II and IV and ref 1, can be used within the Marcus cross relationship (eq 5) to calculate absolute rates of self-exchange of the $[M(\text{DMPE})_3]^{+/2+}$ couples. The results of these calculations are summarized in Table V. For each of the three Ru(III/II) electron transfer partners, the calculated $[\text{Re}(\text{DMPE})_3]^{+/2+}$ self-exchange rate is about twice as large as the rate calculated for the $[\text{Tc}(\text{DMPE})_3]^{+/2+}$ couple (average $k_{\text{ex}}^{\text{Re}}/k_{\text{ex}}^{\text{Tc}} = 2.2 \pm 0.9$). From these calculations, reasonable estimates for the $[\text{Re}(\text{DMPE})_3]^{+/2+}$ and $[\text{Tc}(\text{DMPE})_3]^{+/2+}$ self-exchange rates are 4×10^6 and $2 \times 10^6 \text{ M}^{-1} \text{ s}^{-1}$ respectively at 25 °C and 0.10 M ionic strength.

Activation Parameters. The activation parameters listed in Table II are derived from only limited data and therefore cannot be interpreted in too much detail. However, even within the relatively large experimental uncertainties, there appear to be some well-defined qualitative results. (1) As the nature of the Ru(III) oxidant is varied, the observed enthalpies of activation reflect the thermodynamic driving force of the reactions. For either the Tc or Re couples, the equilibrium constants for the reaction decrease in the order $\text{isn} > \text{py} > \text{pic}$ (Table IV) while the corresponding activation enthalpies increase in the order $\text{isn} < \text{py} < \text{pic}$. (2) This trend of decreasing activation enthalpy with increasing driving force does not hold as the nature of the M(I) reductant is varied.

(18) A reviewer has noted that the uncertainties in the calculated ratios might be even larger than anticipated since in the Re system the two bond lengths are both derived from EXAFS data while in the Tc system one bond length is derived from EXAFS and the other is crystallographically derived.

Even though Re(I) is a more powerful reductant than Tc(I) (Table IV), for both the pic and py reactions the activation enthalpy for the Re(I) reduction is larger than that for the Tc(I) reduction. (The large experimental uncertainties associated with the isn reactions make a comparison in this case impossible.) (3) The unfavorable activation enthalpies observed for the Re(I) reductions in the pic and py systems are more than compensated for by very favorable entropies of activation. In these two cases the ΔS^* governing the Re(I) reduction is 10–15 eu more positive than that governing the Tc(I) reduction. (4) This difference in activation entropies disappears for the isn system, possibly because the isonicotinamide complex contains a polar amide group that strongly interacts with the solvent. This amide group could impose significantly different solvent reorganization requirements on the activation complex than are imposed by the nonpolar peripheries of the pyridine and picoline ligands.

Conclusions. The relative self-exchange rate of the $[\text{Tc}(\text{DMPE})_3]^{+/2+}$ and $[\text{Re}(\text{DMPE})_3]^{+/2+}$ couples is adequately described by the Marcus formalism. The above calculations show that the kinetically observed, slightly greater rate of self-exchange of the $[\text{Re}(\text{DMPE})_3]^{+/2+}$ couple is due entirely to the somewhat smaller structural distortions suffered by the inner coordination sphere of the Re complex during electron transfer. The $[\text{Re}(\text{DMPE})_3]^{+/2+}$ couple should be very useful in characterizing the kinetics of other systems because (1) it is easily prepared from readily available, nonradioactive materials,⁶ (2) it is soluble in water and in a variety of polar organic solvents,⁶ (3) it is stable in both acidic and alkaline media, (4) its $E^{\circ'}$ value is accessible to a variety of reagents, (5) it undergoes simple outer-sphere electron transfer, and (6) its self-exchange rate is relatively rapid ($k_{\text{ex}}^{\text{Re}} = 4 \times 10^6 \text{ M}^{-1} \text{ s}^{-1}$) because of the small reorganizational barrier inherent to a d^6/d^5 system.¹

Acknowledgment. Financial support was provided in part by the National Institutes of Health, Grants No. HL-21276 and GM35404. A portion of this work was performed under the auspices of the Office of Basic Energy Sciences, Division of Chemical Sciences, U.S. Department of Energy, under Contract No. W-31-109-ENG-38. EXAFS experiments were conducted at SSRL, which is supported by the Office of Basic Energy Sciences, Department of Energy, and the Biotechnology Resource Program, Division of Research Resources, National Institutes of Health. We are grateful to Dr. J. Kirchhoff and Professor W. R. Heineman for conducting the electrochemical measurements.

Supplementary Material Available: Table A, containing observed rate parameters as a function of temperature, L, $[\text{Re}(\text{I})]_0$, and $[\text{Ru}(\text{III})]_0$ (3 pages). Ordering information is given on any current masthead page.